IEEE Photonics Journal
An IEEE Photonics Society Publication

Optical Multipath RF Self-Interference Cancellation Based on Phase Modulation for Full-Duplex Communication

Volume 12, Number 4, August 2020

Xinxin Su
Xiuyou Han, *Member, IEEE*
Shuanglin Fu
Shuo Wang
Chao Li
Qinggui Tan
Ge Zhu
Chao Wang, *Member, IEEE*
Zhenlin Wu
Yiying Gu
Mingshan Zhao

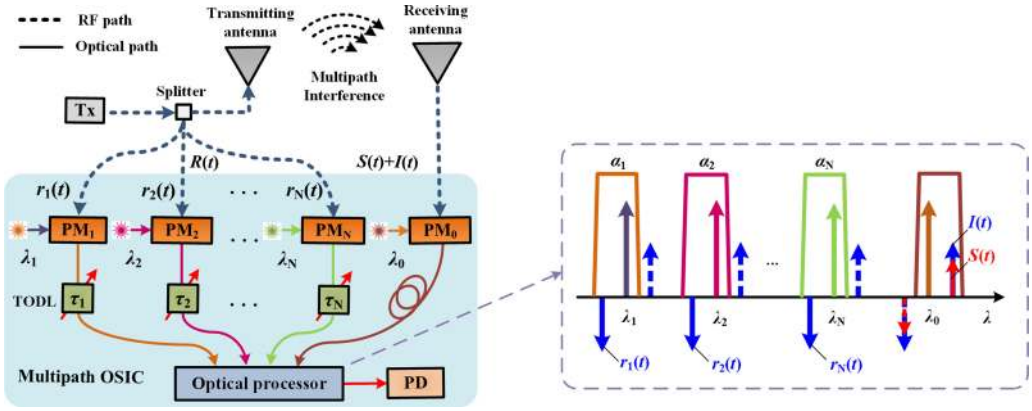

DOI: 10.1109/JPHOT.2020.3002856

Optical Multipath RF Self-Interference Cancellation Based on Phase Modulation for Full-Duplex Communication

Xinxin Su,[1] **Xiuyou Han**,[1] ***Member, IEEE***, **Shuanglin Fu**,[1] **Shuo Wang**,[1] **Chao Li**,[1] **Qinggui Tan**,[2] **Ge Zhu**,[2] **Chao Wang**,[3] ***Member, IEEE***, **Zhenlin Wu**,[1] **Yiying Gu**,[1] **and Mingshan Zhao** [1]

[1]School of Optoelectronic Engineering and Instrumentation Science, Dalian University of Technology, Dalian 116024, China
[2]National Key Laboratory of Science and Technology on Space Microwave, Xi'an 710000, China
[3]School of Engineering and Digital Arts, University of Kent, Canterbury CT2 7NT, U.K.

DOI:10.1109/JPHOT.2020.3002856

Manuscript received May 8, 2020; revised June 9, 2020; accepted June 11, 2020. Date of publication June 16, 2020; date of current version June 30, 2020. This work was supported in part by National Key R&D Program of China under Grant 2019YFB2203202, in part by the National Science Foundation of China under Grants 61875028, 61704017, and 61605023, in part by the Program for Innovative Talents in Universities of Liaoning Province under Grant LR2019017, in part by the Dalian Science and Technology Innovation Foundation under Grant 2018J11CY006, and in part by the Fundamental Research Funds for the Central Universities under Grants DUT18ZD106, DUT18GF102, and DUT18LAB20.
Corresponding author: Xiuyou Han (e-mail: xyhan@dlut.edu.cn)

Abstract: Optical multipath RF self-interference cancellation (SIC) based on phase modulation for full-duplex communication is proposed and demonstrated experimentally. Phase modulation is utilized to convert the RF signal into optical domain, in which the time delay tuning, amplitude tuning and phase inversion for multipath RF SIC are completed. The comprehensive theoretical model of the optical multipath RF SIC system is established, and the factors affecting SIC performance including the time delay, amplitude and phase deviations are analyzed. The experimental results verify the feasibility of the proposed scheme for full-duplex communication with the cancellation depth of 26 dB and 28 dB over 100 MHz at central frequency of 6 GHz and 10 GHz, respectively. A figure of merit of the maximum interference to signal of interest ratio is defined to characterize the SOI recovery capability of optical RF SIC system.

Index Terms: Full-duplex communication, multipath RF self-interference cancellation, phase modulation.

1. Introduction

Compared with time division duplex (TDD) and frequency division duplex (FDD), full-duplex can realize simultaneous transmitting and receiving signals at the same frequency band, which significantly increases spectrum utilization and doubles data rate. Full-duplex has wide potential applications in the new generation mobile communications and the satellite data transmissions [1]–[4]. However, during the full-duplex communication, the transmitted high power signal due to the arrangement of the antenna or the like may cause interference in the same frequency band of the received weak useful signal, which is called RF self-interference or co-location interference,

and cannot be filtered out by a notch filter or a narrow bandpass filter [5], [6]. Therefore, RF self-interference cancellation (SIC) is very urgent for realizing the full-duplex communication. Compared to the electrical technology, the RF SIC technology based on the optical method has the advantages of wide bandwidth, high time delay tuning precision and anti-electromagnetic interference, exhibiting a promising solution for RF self-interference cancellation.

The key to achieving interference cancellation is to provide a reference signal that has the same magnitude and opposite phase of the interference signal with time matching. The cancellation can be achieved by using two Mach-Zehnder modulators (MZMs) biased at the opposite orthogonal bias points [7], [8] or dual-drive MZM [9], [10], dual-parallel MZM [11]–[13] operating at the proper bias points to obtain the out-of-phase relationship. However, DC bias control increases the complexity of the system and may affect the operation stability. Phase-reversion can also be achieved by a Balun as the RF power splitter at the input port [14] or a balanced photo detector as the RF power combiner at the output end [15]–[17]. In these schemes, the amplitude and time matching of the reference signal is realized by the variable optical attenuator (VOA) and the tunable optical delay line (TODL). In addition, the amplitude and time of reference signal can also be adjusted by using the gain and slow light effect of the semiconductor optical amplifiers (SOAs) [18], which has the potential advantage of fully photonic integration on a chip with a compact sub-system and low power consumption [19], [20]. However, due to the dependent relationship between the gain and slow light effect, the tunable range of the amplitude and time delay with the cascaded SOAs may be degraded as the frequency increases.

In real scenario, the interference from the transmitting antenna to the receiving antenna is a combined result of direct path coupling between the transmitter and receiver as well as multiple reflection, scattering and diffraction through different paths. This is called multipath interference, which must be resolved for the realization of full-duplex communication. For multipath interference cancellation, multiple replicas of the reference signal are produced by using an optical splitter and transmit through different optical delay and amplitude attenuation [21], [22]. Then a single-mode to multi-mode (SM-MM) combiner is utilized to combine the multiple replicas of the reference signal and received interference signal into the photo detector to complete the cancellation. The scalability of the optical SIC system may be limited by the number of orthogonal spatial modes that can be multiplexed by the SM-MM combiner [23], which is not an easily-achievable device. In [24] a scheme based on two polarization modulators and a dispersive element is proposed and demonstrated for multipath interference cancellation. Multiple optical compensation branches are formed by an array of tunable lasers. By adjusting the wavelength and the optical power of each tunable laser, the multipath reference can be reconstructed for counter-phase cancellation with delay and amplitude matching. However, the polarization state may be affected by the environmental conditions and the system stability may be degraded. Fiber Bragg grating (FBG) based optical delay lines are designed and fabricated for providing a large number of delay taps in [25], [26], which can achieve multipath cancellation with a high delay spread and low insertion loss. It is a unique design but the time delay tuning is discrete by now.

By virtue of the inherent out-of-phase relationship between the two sidebands of the phase-modulated signal, we proposed an optical RF SIC method based on phase modulation and optical sideband filtering for full-duplex application [27]. It has the advantages of simple and stable system structure with no need of bias point control. The preliminary experimental results demonstrate the feasibility of the scheme. However, the capability for multipath RF SIC and the recovery of signal of interest (SOI) has not been investigated. In this paper, we present a multipath RF SIC scheme by utilizing an optical spectrum shaping technique, where the amplitude tuning and sideband filtering are realized completely by only one optical engine based on diffraction grating and solid-state liquid crystal on silicon (LCoS). The comprehensive model of the optical multipath RF SIC system is established to analyze the factors affecting the RF SIC performance, including the time delay deviation, amplitude deviation, and phase deviation. The experiment of optical multipath interference cancellation for full-duplex communication is also carried out with the consistency of measured results compared with the simulated ones. The recovery of SOI with 16-QAM modulation on RF carrier of 6 GHz is investigated experimentally. And a figure of merit of the interference to

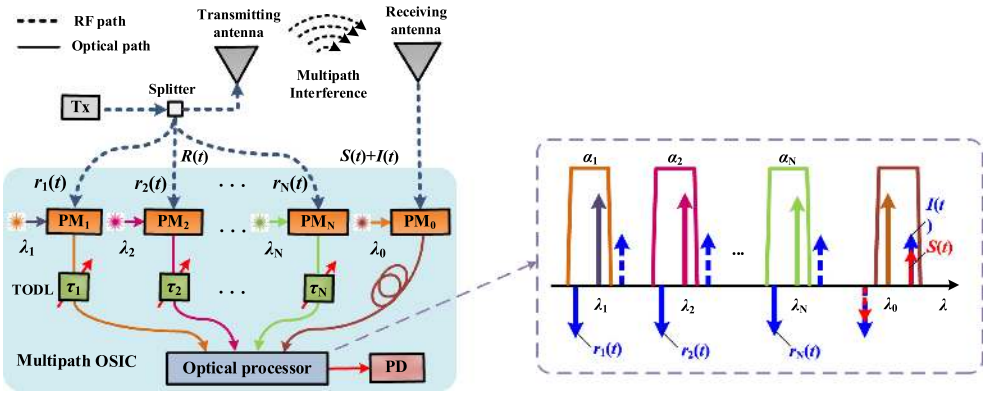

Fig. 1. The schematic of the optical multipath RF SIC system based on phase modulation. The dashed block shows the sideband filtering and amplitude tuning in the optical processor. PM, phase modulator; TODL, tunable optical delay line; PD, photo detector; Tx, transmitter.

SOI ratio is defined for the first time as far as we know to characterize the capability of optical RF SIC system for full-duplex communication.

2. Operation Principle and Performance Analysis

The multipath optical RF SIC system based on phase modulation is shown in Fig. 1. The received RF signals $S(t) + I(t)$ from the receiving antenna are modulated on the lightwave of λ_0 via the phase modulator PM_0, where $S(t)$ is the SOI and $I(t)$ is the multipath interference signal, which can be expressed as

$$I(t) = \sum_{n=1}^{N} i_n(t), (n = 1, 2, \ldots, N) \tag{1}$$

where $i_n(t)$ is the n^{th} path component of the self-interference. The reference RF signals of $r_1(t)$, $r_2(t)$, $r_3(t)$, …, $r_N(t)$ are split from the transmitter (Tx) and modulated on the lightwaves of λ_1, λ_2, …, λ_N via PM_1, PM_2, …, PM_N, respectively. The time delay of each path can be adjusted by the tunable optical delay lines (TODLs). The phase-modulated reference and received signals are input to an optical processor with the function of sideband filtering and amplitude tuning as the dashed block shown in Fig. 1. The optical processor is based on diffraction grating and LCoS [28]. The processed signals from the optical processor are input to a photo detector (PD). The operation principle and the cancellation performance are analyzed as follows.

2.1 Operation Principle

The operation principle of the proposed scheme for multipath interference cancellation is to adjust the phase, amplitude and delay of the electro-optic phase-modulated RF signals in optical domain, by which the reference signal cancel the corresponding interference signal in each path. In order to understand the operation process, the n^{th} path interference cancellation is deduced mathematically, and the multipath interference cancellation can be generalized accordingly.

For the n^{th} interference signal, it is converted into optical domain via the electro-optic phase modulator PM_0. The output phase-modulated signal can be expressed as

$$E_{out-i,n}(t_{i,n}) = E_0 e^{j2\pi f_0 t_{i,n}} e^{j\frac{\pi V_{i,n}\cos(2\pi f_{RF} t_{i,n})}{V_{\pi 0}}} \tag{2}$$

where E_0 and f_0 are the amplitude and the frequency of the optical carrier from the laser of λ_0, $V_{i,n}$ and f_{RF} are the voltage and frequency of the n^{th} interference RF signal, $V_{\pi 0}$ is the half-wave voltage

of PM_0. The n^{th} reference signal is also converted into optical domain via the electro-optic phase modulator PM_n. The output phase-modulated signal can be expressed as

$$E_{out-r,n}(t_{r,n}) = E_n e^{j2\pi f_n t_{r,n}} e^{j\frac{\pi V_{r,n}\cos(2\pi f_{RF} t_{r,n})}{V_{\pi n}}} \tag{3}$$

where E_n and f_n are the amplitude and the frequency of the optical carrier from the laser of λ_n, $V_{r,n}$ is the voltage of the n^{th} reference RF signal. $V_{\pi,n}$ is the half-wave voltage of PM_n.

By using the Jacobi–Anger expansions, (2) and (3) can be expressed as

$$E_{out-i,n}(t_{i,n}) = E_0\left(J_{-1}(m_{i,n})e^{j[2\pi(f_0-f_{RF})t_{i,n}-\frac{\pi}{2}]} + J_0(m)e^{j2\pi f_0 t_{i,n}} + J_1(m_{i,n})e^{j[2\pi(f_0+f_{RF})t_{i,n}+\frac{\pi}{2}]}\right) \tag{4}$$

$$E_{out-r,n}(t_{r,n}) = E_n\left(J_{-1}(m_{r,n})e^{j[2\pi(f_n-f_{RF})t_{r,n}-\frac{\pi}{2}]} + J_0(m_{r,n})e^{j2\pi f_n t_{r,n}} + J_1(m_{r,n})e^{j[2\pi(f_n+f_{RF})t_{r,n}+\frac{\pi}{2}]}\right) \tag{5}$$

where J_0, J_1, J_{-1} are the 0 and $\pm1^{st}$ order Bessel function of the first kind, $m_{i,n} = \pi V_{i,n}/V_{\pi 0}$ and $m_{r,n} = \pi V_{r,n}/V_{\pi n}$ are the modulation indexes. When deriving (4) and (5), the 0 and $\pm1^{st}$ order components are considered.

The n^{th} optically carried reference signal is input to the n^{th} TODL with an added time delay of τ_n. And then it is processed by the optical processor with the amplitude tuning of α_n and the right sideband being filtered out as the dashed block shown in Fig. 1. And the left sideband of the optically carried n^{th} interference signal is filtered out by the optical processor. Then the output optically carried n^{th} interference signal and reference signal can be expressed as

$$E_{out-i,n}(t_{i,n}) = E_0\left(J_{-1}(m_{i,n})e^{j[2\pi(f_0-f_{RF})t_{i,n}-\frac{\pi}{2}]} + J_0(m)e^{j2\pi f_0 t_{i,n}}\right) \tag{6}$$

$$E_{out-r,n}(t_{r,n}+\tau_n) = \alpha_n E_n\left(J_0(m_{r,n})e^{j2\pi f_n(t_{r,n}+\tau_n)} + J_1(m_{r,n})e^{j[2\pi(f_n+f_{RF})(t_{r,n}+\tau_n)+\frac{\pi}{2}]}\right) \tag{7}$$

These single sideband with optical carrier (SSB+C) signals are fed to the PD, upon which the optoelectronic conversion is conducted and the output current can be expressed as

$$i_{out-i,n}(t_{i,n}) = -\rho E_0 J_0(m_{i,n})J_1(m_{i,n})\cos\left(2\pi f_{RF} t_{i,n} + \frac{\pi}{2}\right) \tag{8}$$

$$i_{out-r,n}(t_{r,n}+\tau_n) = \rho\alpha_n E_n J_0(m_{r,n})J_1(m_{r,n})\cos\left[2\pi f_{RF}(t_{r,n}+\tau_n) + \frac{\pi}{2}\right] \tag{9}$$

where ρ is the responsivity of the PD. From (8) and (9), it can be seen that the two output signals have the opposite phase due to the inherent out-of-phase relationship between the two sidebands of phase modulated signal [29]. According to (8) and (9), if the following two conditions are matched, the n^{th} interference signal can be cancelled by the n^{th} reference signal.

$$E_0 J_0(m_{i,n})J_1(m_{i,n}) = \alpha_n E_n J_0(m_{r,n})J_1(m_{r,n}) \tag{10}$$

$$t_{i,n} = t_{r,n} + \tau_n \tag{11}$$

The two conditions can be realized by adjusting the amplitude of α_n in the n^{th} channel by the optical processor and the time delay of τ_n by the n^{th} TODL.

For the multiple interference cancellation, the total output from the PD can be expressed as

$$y(t) = S(t) + I(t) + R(t) = S(t) + \sum_{n=1}^{N} i_{out-i,n}(t_{i,n}) + \sum_{n=1}^{N} i_{out-r,n}(t_{r,n}+\tau_n) \tag{12}$$

where $i_{out-i,n}(t_{i,n})$ and $i_{out-r,n}(t_{r,n}+\tau_n)$ are output current from the PD of the n^{th} interference signal and the n^{th} reference signal processed by the optical processor and the TODLs, respectively, as expressed in (8) and (9). When the amplitude and time of each reference signal are properly controlled and the conditions in (10) and (11) are matched, the multipath interference can be cancelled and the SOI is recovered.

The interference cancellation depth is one of the important parameters to characterize the performance of optical RF SIC system, which is affected by the time delay, amplitude and phase

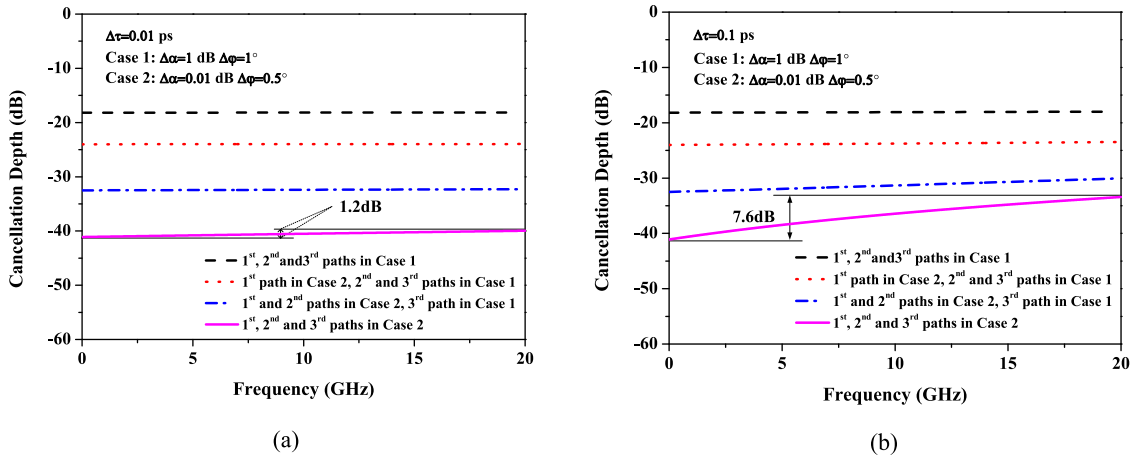

Fig. 2. Multipath self-interference cancellation performance with different mismatching states, (a) $\Delta\tau =$ 0.01 ps and (b) $\Delta\tau = 0.1$ ps.

deviations between the reference path and the interference path. Therefore, the cancellation depth *CD* is defined as the average power ratio before and after the interference cancellation system, and expressed as

$$CD = \frac{\frac{1}{T}\int_0^T \left|\sum_{n=1}^{N} i_{out-i,n}(t_{i,n}) + \sum_{n=1}^{N} i_{out-r,n}(t_{r,n}+\tau_n)\right|^2 dt}{\frac{1}{T}\int_0^T \left|\sum_{n=1}^{N} i_{out-i,n}(t_{i,n})\right|^2 dt} \tag{13}$$

In the actual application process, the conditions expressed as (10) and (11) for the multipath interference cancellation may not be achieved completely. For the nth pair of reference and interference signals, the amplitude, time delay and phase deviations between the two paths are indicated as $\Delta\alpha_n$, $\Delta\tau_n$, and$\Delta\varphi_n$, respectively. According to the Parseval theorem [30], the energy value of the signal with a certain bandwidth of B in the frequency domain is described as $\int_{f_0-B/2}^{f_0+B/2} |I(f)|^2 df$. The cancellation depth *CD* for the multipath optical SIC with a certain bandwidth of B can be expressed as

$$CD\left(\Delta\alpha_n, \Delta\tau_n, \Delta\varphi_n, B\right) = \frac{\int_{f_0-\frac{B}{2}}^{f_0+\frac{B}{2}} \left|\sum_{n=1}^{N} \left(\mathrm{I}_{\mathrm{out-i,n}}(f) - 10^{\frac{\Delta\alpha_n}{20}} e^{j2\pi f\Delta\tau_n} e^{j\Delta\varphi_n} \mathrm{I}_{\mathrm{out-r,n}}(f)\right)\right|^2 df}{\int_{f_0-\frac{B}{2}}^{f_0+\frac{B}{2}} \left|\sum_{n=1}^{N} \mathrm{I}_{\mathrm{out-i,n}}(f)\right|^2 df} \tag{14}$$

As a result, the model for multipath optical RF SIC system is established.

2.2 Cancellation Performance Analysis

According the above established model, the cancellation performance of the multipath optical SIC system affected by the amplitude, time delay and phase deviation is analyzed. Here, N is selected as 3 and the normalized power distribution of three-path interference signals are 0.5, 0.33 and 0.17, respectively. Certainly, it can be extended to a large number of paths with arbitrary power distribution. The delay deviation is set to be 0.01ps and two cases are considered for amplitude and phase deviations. Case 1 is with the amplitude deviation of 1dB and the phase deviation of 1°. Case 2 is with the amplitude deviation of 0.01dB and the phase deviation of 0.5°. When the mismatch between each reference and interference paths are all set in Case 1, the simulated result is shown as the black dash line in Fig. 2(a) with the cancellation depth of about 17 dB. Then the mismatch in the two reference paths are set in different states and the simulated results are also shown in Fig. 2(a). The cancellation depth will be deeper when the amplitude and phase deviation between

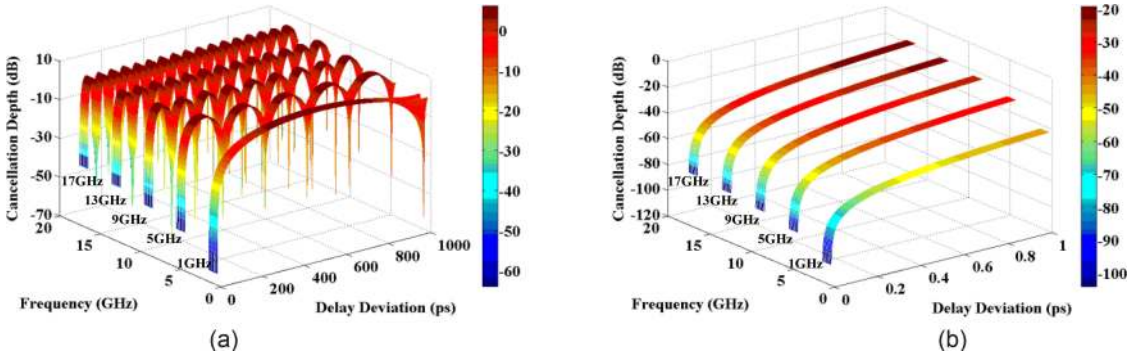

Fig. 3. Cancellation depth at different frequencies with time delay deviation within (a) 1000 ps and (b) 1 ps.

each reference and interference paths becomes smaller. The cancellation depth of about -41 dB is achieved as the mismatch between each reference and interference paths are all in Case 2. There is a small difference of the cancellation depth over the frequency band. The cancellation depth at 1kHz is 1.2 dB higher than the one at 20 GHz. In order to further characterize the cancellation depth with frequency dependence, the simulation is conducted with the delay deviation of $\Delta\boldsymbol{\tau} = 0.1$ps and the similar states in Fig. 2(a) and the results are shown in Fig. 2(b). It can be seen that when the amplitude deviation and the phase deviation decrease the cancellation depth is not flat over the whole frequency band. As the purple cure shown in Fig. 2(b), the cancellation depth is about -41 dB at 1 kHz and -33.4 dB at 20 GHz, with a difference of 7.6 dB. Therefore, when the delay deviation is relatively large, the frequency-dependent response occurs.

Then, the impact of the three influencing factors on the multipath optical RF SIC system is analyzed. It is considered that the multiplexed reference paths have the same delay, amplitude, phase deviation value, where the delay and amplitude depend on the minimum adjustment accuracy of the tunable optical delay lines and the amplitude regulators. As expressed in (15), it is generally considered that only delay deviation or phase deviation should be considered, but this can only be applied to a single frequency. For full-duplex communication, the transmitted signal has a certain bandwidth and the obtained phase value is different for each frequency by changing the delay. Therefore, it is necessary to consider both delay deviation and phase deviation under a certain bandwidth.

$$\Delta\varphi = 2\pi f \Delta\tau \tag{15}$$

2.2.1 The Time Delay Deviation: The effects of time delay deviation on interference cancellation depth is investigated. During the simulation, the amplitude is assumed as being matched, and the phase deviation is 0°. The cancellation depth with time delay deviation within 1000 ps at different center frequencies with the bandwidth of 1 GHz are shown in Fig. 3(a). It can be seen that the cancellation depth is changed periodically with different time delay deviation for a certain center frequency, and the period becomes shorter as the center frequency increases. It is because that the phase of the optical carried RF signal changes with a period of 2π as the time delay deviation increases. As shown in Fig. 3(a), the interference over the bandwidth can be suppressed in the first period. Only the single frequency at the center of the wideband signal can be cancelled completely in every period, while other frequencies cannot be suppressed well in the second and following periods. Therefore, in order to obtain the interference cancellation over a wide band the delay deviation should be kept within the first period, and then the phase adjustment is applied.

In order to explore the influence of the time delay deviation on cancellation depth in one period, the max time delay deviation is set as 1 ps, and the simulated results are given in Fig. 3(b). It can be seen that the cancellation depth becomes deeper with decreasing delay deviation. For the same time delay deviation, the cancellation depth deteriorates when the center frequency increases.

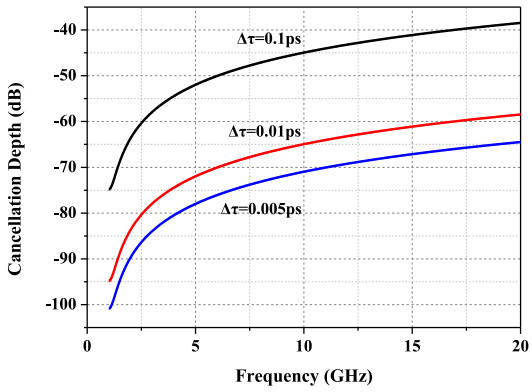

Fig. 4. Cancellation depth with RF frequency at different adjustment accuracy of time delay.

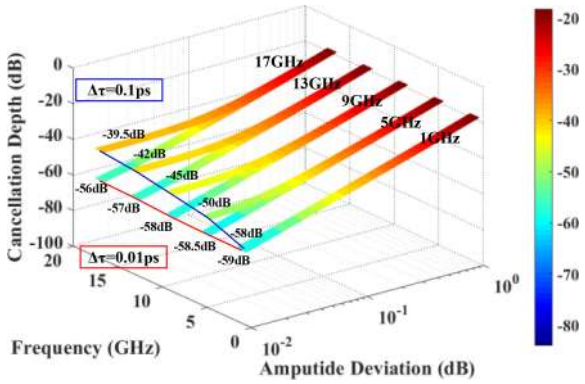

Fig. 5. The effect of amplitude mismatch on cancellation depth at different frequencies (blue line indicates delay mismatch of 0.1 ps, red line indicates delay mismatch of 0.01 ps).

Therefore, the smaller time delay deviation is needed for higher frequency to achieve the same cancellation depth.

In the practical system, the time delay deviation is determined by the adjustment accuracy of the tunable optical delay line. The cancellation depth with the adjustment accuracy of 0.1 ps, 0.01 ps and 0.005 ps is simulated and the results are shown in Fig. 4. For a certain frequency, the cancellation depth is enhanced with the time delay adjustment accuracy being improved. For example, for the frequency of 10 GHz, the cancellation depth is −45 dB, −65 dB and −71 dB for the adjustment accuracy of 0.1 ps, 0.01 ps and 0.005 ps, respectively. Therefore, the tunable optical delay line with higher adjustment accuracy is desirable to achieve deeper cancellation depth.

2.2.2 The Amplitude Deviation: Without considering the phase deviation, we get the cancellation depth under different amplitude mismatch when the delay deviation is 0.1ps and 0.01ps, respectively, as shown in Fig. 5. As the magnitude of the amplitude mismatch increases, from 0.01dB to 1dB, the cancellation depth gradually degrades. When the delay mismatch value is changed from 0.1ps to 0.01ps, the variation of the cancellation depth becomes deeper with the amplitude being gradually matched. Moreover, when the delay and amplitude deviations are constant, the cancellation depth will deteriorate as the frequency increases. Therefore, in order to achieve a certain depth of cancellation, the required tuning accuracy of the amplitude will increase at higher frequencies.

2.2.3 The Phase Deviation: In the proposed optical RF SIC system, each device in the optical links will bring a certain phase, especially the additional phase generated by the optical processor during optical sideband filtering [31], which may affect the out of phase relationship between the interference link and the reference link. Therefore, the influence of self-interference cancellation

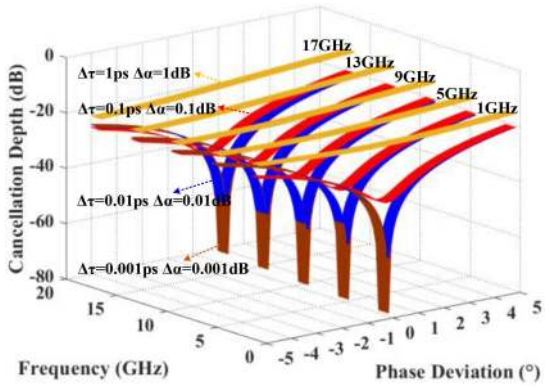

Fig. 6. The effect of phase deviation on the cancellation depth.

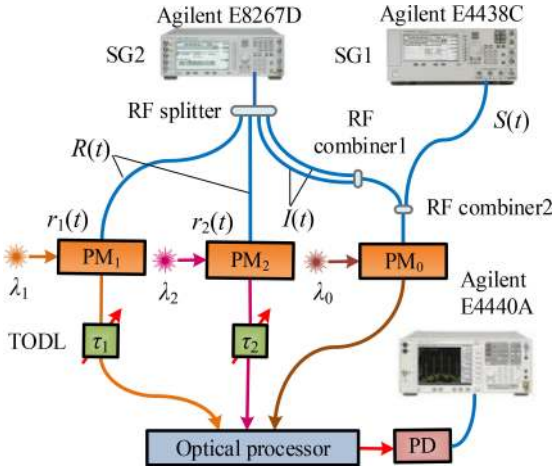

Fig. 7. The experiment setup to demonstrate the optical multipath RF SIC.

by a certain phase deviation is analyzed. Fig. 6 shows the effect of different additional phase on the cancellation depth under different delay and amplitude mismatch. There are four pairs of delay and amplitude mismatch, including (1 ps, 1 dB), (0.1 ps, 0.1 dB), (0.01 ps, 0.01 dB) and (0.001ps, 0.001 dB). It can be seen that as the delay and amplitude mismatch is being smaller, the cancellation depth will become deeper. When the delay mismatch and the amplitude mismatch are smaller than 0.1 ps and 0.1 dB, respectively, the cancellation depth is better than -30 dB, and the phase deviation plays a major role. Smaller phase deviation obtains better self-interference cancellation performance.

3. Multipath Cancellation Experiment and Results

In order to investigate the feasibility of proposed multipath self-interference cancellation system, an experiment is carried out. The experiment setup is shown as Fig. 7 with two-path interference cancellation demonstration, which is limited by the currently available optoelectronic devices in our lab. The SOI $S(t)$ is output from the signal generator (SG1, Agilent E4438C), and the interference signals $I(t)$ and the reference signals $R(t)$ are generated by another signal generator (SG2, Agilent E8267D). Here, two interference signals with different delay and amplitude are used to simulate multipath interference signals in real situation. The signals of interest and the interference signals are modulated on the optical carrier 1548.522 nm (λ_0) in the interference path through PM_0, and the reference signals are converted into optical paths of 1549.350 nm (λ_1) and 1549.858 nm (λ_2)

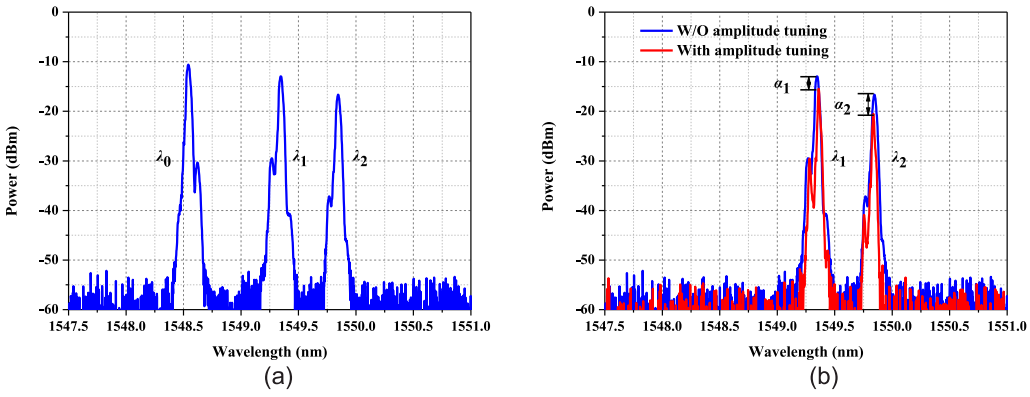

Fig. 8. The optical spectra of the phase-modulated signals by the optical processor, (a) sideband filtering and (b) amplitude tuning ($f_{RF} = 10$ GHz).

through PM_1 and PM_2, respectively. The time delay of the reference paths is adjusted by the $TODL_1$ and $TODL_2$ with time delay accuracy of 0.01 ps and tunable range of 600 ps. The phase modulated signals of the three paths are input into the optical processor (WaveShaper 16000S). The optical processor is programed as three bandpass filters to remove the corresponding sidebands of the three phase-modulated signals as the dashed block shown in Fig. 1. At the same time, the amplitude of the reference signals is adjusted in the optical processor. The output SSB+C signals are input into the PD (Miteq SCMR-10M, 18 GHz). The detected signals from the PD are measured by an electrical spectrum analyzer (ESA, Agilent E4440A).

3.1 Multipath Spectrum Processing

At first, the simultaneous multipath spectrum processing by the optical processor is measured. The RF signal with the frequency of 10 GHz is modulated on the interference and reference optical carriers. Fig. 8(a) shows the optical spectra of the phase-modulated signals output from the optical processor. It can be seen that the left sideband of the interference modulated signal (λ_0) and the right sidebands of the reference modulated signals (λ_1 and λ_2) are filtered out and the SSB+C signals are generated. Fig. 8(b) shows the amplitude tuning of the two reference modulated SSB+C signals with the amplitude adjustment of α_1 and α_2 independently.

3.2 RF Self-Interference Cancellation

The multipath RF self-interference cancellation performance within a certain bandwidth is measured. A 6 GHz single tone signal with the power of -55 dBm from SG1 is used as the SOI. The additive white Gaussian noise (AWGN) from SG2 with a bandwidth of 100 MHz and the power of -2.5 dBm is modulated on the RF signal at 6 GHz, which is utilized as the interference signal. With the laser sources of λ_1 and λ_2 in reference paths being turned off, the output spectrum is measured as shown in Fig. 9(a). It can be seen that a strong interference signal is observed as the red curve. Then the first reference path is established by tuning on the laser source of λ_1. It can be seen from Fig. 9(a), the interference signal is suppressed with the cancellation depth of 15 dB. However, the SOI is still buried in interference signal. After turning on the laser source of λ_2, the two-path interference cancellation system is established, and the measured result is shown as the black curve in Fig. 9(a). The cancellation depth of 26 dB is obtained, and the SOI is recovered. The cancellation performance for the center frequency of 10 GHz is also measured, and the results are shown in Fig. 9(b). It can be seen that the cancellation depth of 17 dB and 28 dB are realized by single path interference cancellation and multipath interference cancellation, respectively, and the recovery of SOI is completed. From Fig. 9(a) and 9(b), it can be seen that there are still some

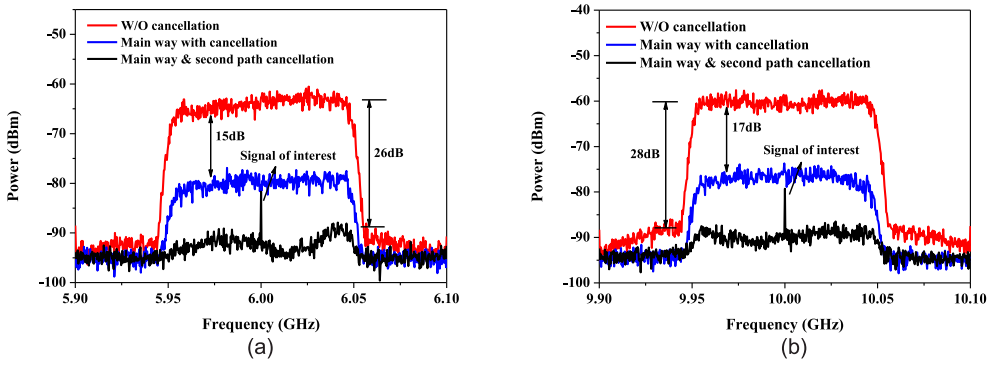

Fig. 9. The output RF spectra in bandwidth of 100 MHz with and without cancellation (a) $f_{RF} = 6$ GHz and (b) $f_{RF} = 10$ GHz.

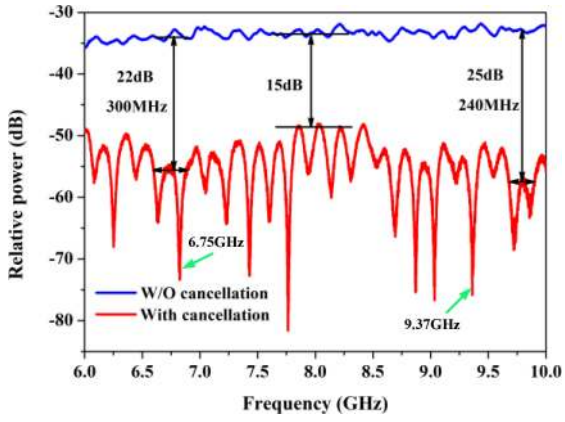

Fig. 10. The measured cancellation depth with and without SIC for larger bandwidth (6∼10 GHz).

residual interference noise after cancellation and the residual interference noise is not uniform within the bandwidth. It is mainly due to the nonidentical amplitude response and phase response between the interference and reference paths.

Then, the RF self-interference cancellation capability for larger bandwidth is investigated by using the vector network analyzer (VNA, Keysight Technologies N5247B) to measure the cancellation depth. For the cancellation of the main path interference, the measured amplitude response from 6 GHz to 10 GHz with and without SIC is shown in Fig. 10. It can be seen that at the central frequency of 9.75 GHz, a cancellation depth of 25 dB is obtained with the bandwidth of 240 MHz. The cancellation of 22 dB is achieved in the bandwidth of 300 MHz at the central frequency of 6.75 GHz. For the whole frequency band of 4 GHz, the cancellation depth is about 15 dB.

In order to analyze the different cancellation depth at the different central frequency, the phase and amplitude response of the interference and the reference paths from 6 GHz to 10 GHz are measured by the VNA and the amplitude and phase difference between the two paths are plotted in Fig. 11. It can be seen that the phase difference shown as the blue curve in Fig. 11 floats up and down around 180°, which indicates that the phase response between the interference and reference paths are opposite basically. The maximum phase deviation is about 14° near the frequency of 8 GHz which induces the relative small cancellation depth of about 15 dB as shown in Fig. 10. The amplitude deviation is about 1.5 dB over the frequency band of 4 GHz shown as the red curve in Fig. 11. When the amplitude response and the phase response between the two paths nearly match, as marked 6.75 GHz and 9.37 GHz in Fig. 11, the maximum cancellation depth is obtained, which is corresponding to the result in Fig. 10. The amplitude mismatch and the phase difference are mainly due to the non-equal amplitude response and additional phase between the

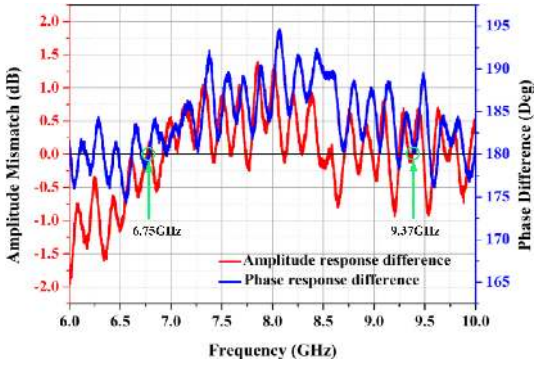

Fig. 11. The amplitude and phase difference between the reference and interference paths.

TABLE 1
Amplitude and Phase Deviations Impacting on RF SIC Performance

CD/dB \ Δα/dB / Δφ/°	0.1	0.2	0.4	0.8	1.6
1	-33.5	-30.7	-25.9	-20.2	-13.8
2	-28.6	-27.5	-24.6	-19.7	-13.7
4	-22.9	-22.6	-21.4	-18.3	-13.3
8	-17	-16.9	-16.5	-15.1	-11.9
16	-11	-10.9	-10.8	-10.3	-8.7

reference path and the interference path caused by the optoelectronic devices in the experimental setup.

Then, the influence of the comprehensive deviation of phase response and amplitude response on the RF self-interference cancellation depth is analyzed. By using Eq. (14), we calculate the cancellation depth with the typical amplitude deviation $\Delta\alpha$ and phase deviation $\Delta\varphi$ obtained from Fig. 11, and the results are listed in Table 1. The cancellation depth becomes deeper with the amplitude and phase deviation being smaller. When the amplitude deviation $\Delta\alpha$ is less than 0.2 dB and the phase deviation $\Delta\varphi$ is less than 1°, the cancellation depth of the system can be lower than -30 dB. In order to obtain the cancellation depth better than -20 dB, $\Delta\alpha$ and $\Delta\varphi$ should be less than 0.4 dB and 4° over the operation bandwidth, respectively. The calculated results are consistent with the measured ones in Fig. 10, which proves the correctness of the theoretical model for the multipath self-interference cancellation.

4. Full-Duplex Communication by Optical RF SIC Technique

The full-duplex communication by using the established optical multipath RF SIC system is measured with the 16-QAM modulation signals on RF carrier of 6 GHz. The test frequency is limited by the measurement equipment in our lab currently.

4.1 SOI Recovery Performance

The 16-QAM signal with a bandwidth of 40 MHz and a power of -20 dBm carried by the RF of 6 GHz from SG1 is used as the SOI. The additive white Gaussian noise (AWGN) from SG2 with a bandwidth of 40 MHz and a power of 17 dBm at the central frequency of 6 GHz is applied as the interference signal. Fig. 12 presents the output spectra and the corresponding constellation diagrams at different interference cancellation states. Fig. 12(a) is the measured spectrum without interference cancellation when the laser source of λ_1 and λ_2 are both turned off. A strong interference signal is observed in the electrical spectrum and the SOI cannot be

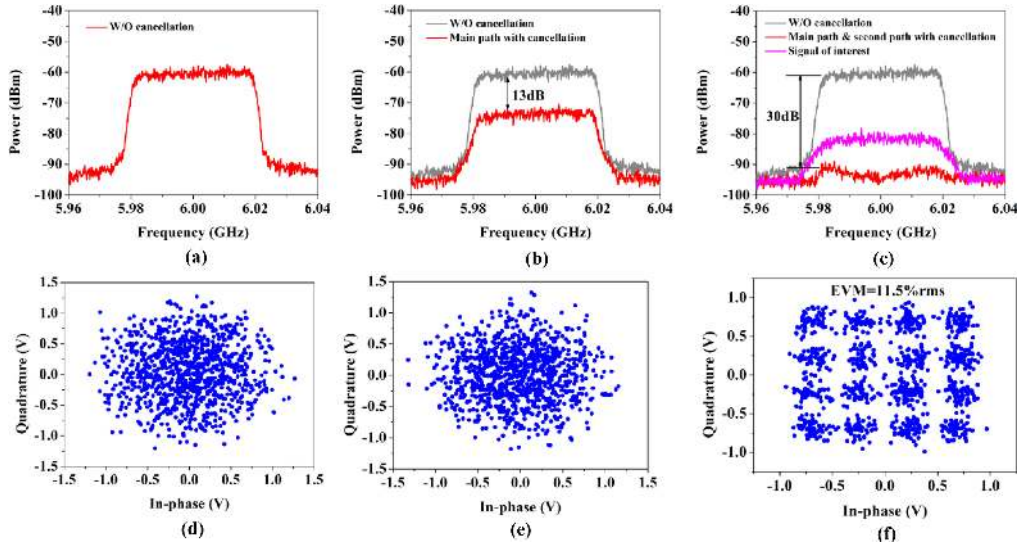

Fig. 12. The measured output spectra and the corresponding constellation diagram. (a) and (d) without interference cancellation, (b) and (e) main path interference with cancellation, (c) and (f) main path & second path interference with cancellation.

recovered as shown in Fig. 12(d). Then, by tuning on the laser source of λ_1, the main interference signal is canceled with a suppression depth of 13 dB as shown in Fig. 12(b). However, the SOI is still embedded in the interference noise and the constellation diagram is not clear as exhibited in Fig. 12(e). After further tuning on the laser source of λ_2, the second interference is suppressed with a total cancellation depth of 30 dB, and the SOI is recovered as the pink curve in Fig. 12(c). The corresponding constellation diagram of 16-QAM signal is clear with an error vector magnitude (EVM) value of 11.5% rms as demonstrated in Fig. 12(f).

4.2 Maximum Interference to SOI Ratio

In order to characterize the SOI recovery capability of the optical RF SIC system, a figure of merit, the maximum interference to SOI ratio for a certain EVM value of the recovered SOI signal during the full-duplex communication, is defined as

$$\eta = \frac{P_{SI}}{P_{SOI}} \tag{16}$$

where P_{SI} is the power of interference signal, and P_{SOI} is the power of signal of interest. Therefore, η represents the capability of the optical RF SIC system to eliminate interference and recover SOI. It is much useful to demonstrate the communication performance of optical RF SIC based full-duplex communication system.

During the measurement, the bandwidth is set as 40 MHz, and the input power of SOI is -17 dBm. After achieving multipath self-interference cancellation, we gradually increase the interference signal power and the corresponding EVM values of the recovered SOI are measured and the results are shown in Fig. 13. With the increase of the interference signal power, the EVM performance degrades. According to the international 3GPP guidelines, the maximum EVM value allowed by 16QAM modulation is 12.5% rms [32]. From Fig. 13 it can be inferred that the maximum interference signal power of the established system is -2 dBm and the corresponding maximum interference to SOI ratio is 15 dB.

The SOI recovery capability of the established optical RF SIC system with the modulation bandwidth of 10, 20, 30, 40 and 50 MHz is also measured. The maximum interference to SOI ratio η is characterized and the results are given in Table 2. The maximum modulation bandwidth

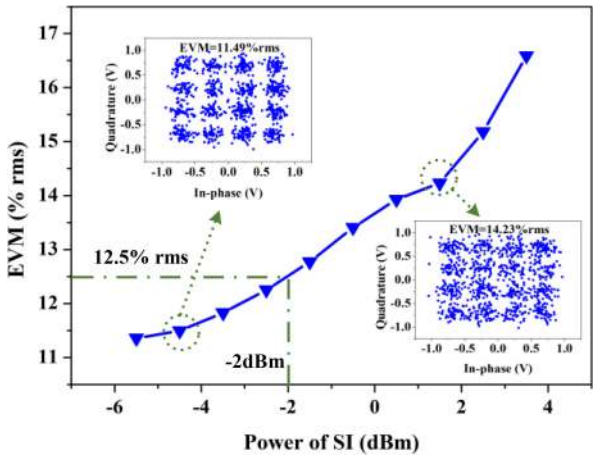

Fig. 13. The measured EVM of the recovered SOI with different power of interference signal.

TABLE 2
The Maximum Interference Signal to SOI ratio η With Different Bandwidths

Bandwidth/MHz	10	20	30	40	50
Power of SI/dBm	2.7	1.4	0.3	-2	-1.7
Power of SOI/dBm	-19	-19	-18	-17	-15
η/dB	21.7	20.4	18.3	15	13.3

is limited by the current measurement equipment in our lab. The maximum interference to SOI ratio η exhibits the operation performance of the established experiment setup for full-duplex communication. Certainly, the value of η is not high enough by now. It can be improved by further combining the digital processing method [33], [34] in the real applications.

5. Conclusion

An optical multipath RF self-interference cancellation scheme based on phase modulation is presented, in which the sideband filtering and amplitude tuning is completed in one optical engine. The influence of the time delay, amplitude and phase deviations between the reference and interference paths on the multipath RF SIC performance are analyzed and simulated. The experiment setup is established and the measured results show that the interference cancellation depth of 26 dB and 28 dB are achieved with the bandwidth of 100 MHz at the center frequency of 6 GHz and 10 GHz, respectively. For a larger bandwidth, the cancellation depth of 25 dB over 240 MHz and 15 dB over the frequency band of 4 GHz are obtained. The full-duplex communication based on the established optical multipath RF SIC is tested. The recovery of SOI with 16-QAM modulation is measured and the maximum interference to SOI ratio is defined to characterize the SOI recovery capability of the optical multipath RF SIC system.

References

[1] A. Sabharwal, P. Schniter, D. Guo, D. W. Bliss, S. Rangarajan, and R. Wichman, "In-band full-duplex wireless: Challenges and opportunities," *IEEE J. Sel. Areas Commun.*, vol. 32, no. 9, pp. 1637–1652, Sep. 2014.

[2] S. K. Sharma, T. E. Bogale, L. B. Le, S. Chatzinotas, X. Wang, and B. Ottersten, "Dynamic spectrum sharing in 5G wireless networks with full-duplex technology: Recent advances and research challenges," *IEEE Commun. Surveys Tut.*, vol. 20, no. 1, pp. 674–707, Jan.–Mar. 2018.

[3] M. Jain *et al.*, "Practical, real-time, full duplex wireless," in *Proc. [C] 17th Annu. Int. Conf. Mobile Comput. Netw.*, 2011, pp. 301–312.

[4] J. I. Choi, M. Jain, K. Srinivasan, P. Levis, and S. Katti, "Achieving single channel, full duplex wireless communication," *[C] Proc.16th Annu. Int. Conf. Mobile Comput. Netw.* 2010, pp. 1–12.

[5] S. Hong *et al.*, "Applications of self-interference cancellation in 5G and beyond," *IEEE Commun. Mag.*, vol. 52, no. 2, pp. 114–121, Feb. 2014.

[6] K. E. Kolodziej, B. T. Perry and J. S. Herd, "In-band full-duplex technology: Techniques and systems survey," *IEEE Trans. Microw. Theory Techn.*, vol. 67, no. 7, pp. 3025–3041, Jul. 2019.

[7] J. Suarez, K. Kravtsov, and P. R. Prucnal, "Incoherent method of optical interference cancellation for radio-frequency communications," *IEEE J. Quantum Electron.*, vol. 45, no. 4, pp. 402–408, Apr. 2009.

[8] Z. Y. Tu, A. J. Wen, X. R. Li, and H. X. Zhang, "A photonic pre-distortion technique for RF self-interference cancellation," *IEEE Photon. Technol. Lett.*, vol. 30, no. 14, pp. 1297–1300, Jul. 2018.

[9] Y. H. Zhang, S. L. Xiao, H. L. Feng, L. Zhang, Z. Zhou, and W. S. Hu, "Self-interference cancellation using dual-drive Mach-Zehnder modulator for in-band full-duplex radio-over-fiber system," *Opt. Express*, vol. 23, no. 26, pp. 33205–33213, Dec. 2015.

[10] S. Zhu, M. Li, N. H. Zhu, and W. Li, "Photonic radio frequency self-Interference cancellation and harmonic down-conversion for in-band full-duplex radio-over-fiber system," *IEEE Photon. J.*, vol. 11, no. 5, Apr. 2019, Art. no. 5503110.

[11] X. Y. Han, B. F. Huo, Y. C. Shao, and M. S. Zhao, "Optical RF self-interference cancellation by using an integrated dual-parallel MZM," *IEEE Photon. J.*, vol. 9, no. 2, Apr. 2017, Art.no. 5501308.

[12] Y. Chen, and S. L. Pan, "Simultaneous wideband radio-frequency self-interference cancellation and frequency down-conversion for in-band full-duplex RoF systems," *Opt. Lett.*, vol. 43, no. 13, pp. 3124–3127, Jul. 2014.

[13] X. Li *et al.*, "Optimized self-interference cancellation based on optical dual-parallel MZM for co-frequency and co-time full duplex wireless communication under nonlinear distortion and emulated multipath effect," *Opt. Express*, vol. 27, no. 26, pp. 37286–37297, Dec. 2019.

[14] Q. Zhou, H. L. Feng, G. Scott, and M. P. Fok, "Wideband co-site interference cancellation based on hybrid electrical and optical techniques," *Opt. Lett.*, vol. 39, no. 22, pp. 6537–6540, Nov. 2014.

[15] M. P. Chang, M. Fok, A. Hofmaier, and P. R. Prucnal, "Optical analog self-interference cancellation using electro-absorption modulators," *IEEE Microw. Wireless Components Lett.*, vol. 23, no. 2, pp. 99–101, Feb. 2013.

[16] S. J. Zhang, S. L. Xiao, Y. H. Zhang, H. L. Feng, L. Zhang, and Z. Zhou, "Directly modulated laser based optical radio frequency self-interference cancellation system," *Opt. Eng.*, vol. 55, no. 2, Feb. 2016, Art. no. 026116.

[17] L. Huang, Y. H. Zhang, S. L. Xiao, L. Z. Zheng, and W. S. Hu, "Real-time adaptive optical self-interference cancellation system for in-band full-duplex transmission," *Opt. Commun.*, vol. 437, no. 15, pp. 259–263, Apr. 2019.

[18] M. P. Chang, C. Lee, B. Wu, and P. R. Prucnal, "Adaptive optical self-interference cancellation using a semiconductor optical amplifier," *IEEE Photon.Technol. Lett.*, vol. 27, no. 9, pp. 1018–1021, May 2015.

[19] M. P. Chang, E. C. Blow, J. J. Sun, M. Z. Lu, and P. R. Prucnal, "Integrated microwave photonic circuit for self-interference cancellation," *IEEE Trans. Microw. Theory Techn.*, vol. 65, no. 11, pp. 4493–4501, Nov. 2017.

[20] M. P. Chang, E. C. Blow, M. Z. Lu, J. J. Sun, and P. R. Prucnal, "RF characterization of an integrated microwave photonic circuit for self-interference cancellation," *IEEE Trans. Microw. Theory Techn.*, vol. 66, no. 1, pp. 596–605, Jan. 2018.

[21] J. Chang and P. R. Prucnal, "A novel analog photonic method for broadband multipath interference cancellation," *IEEE Microw. Wireless Components Lett.*, vol. 23, no. 7, pp. 377–379, Jul. 2013.

[22] J. J. Sun, M. P. Chang, and P. R. Prucnal, "Demonstration of over-the-air RF self-interference cancellation using an optical system," *IEEE Photon. Technol. Lett.*, vol. 29, no. 4, pp. 397–400, Feb. 2017.

[23] D. Chapman, "Low-loss many-to-one fiber couplers with few or single-mode inputs and a multi-mode output," *Fiber Integr. Opt.*, vol. 23, no. 5, pp. 375–385, 2004.

[24] W. Zhou, P. Xiang, Z. Niu, M. Wang, and S. Pan, "Wideband optical multipath interference cancellation based on a dispersive element," *IEEE Photon. Technol. Lett.*, vol. 28, no. 8, pp. 849–851, Apr. 2016.

[25] K. E. Kolodziej, S. Yegnanarayanan, and B. T. Perry, "Photonic-enabled RF canceller for wideband in-band full-duplex wireless systems," *IEEE Trans. Microw. Theory Techn.*, vol. 67, no. 5, pp. 1–11, May 2019.

[26] K. E. Kolodziej, S. Yegnanarayanan, and B. T. Perry, "Fiber Bragg grating delay lines for wideband self-interference cancellation," *IEEE Trans. Microw. Theory Techn.*, vol. 67, no. 10, pp. 1–10, Oct. 2019.

[27] X. Y. Han, B. F. Huo, Y. C. Shao, C. Wang, and M. S. Zhao, "RF self-interference cancellation using phase modulation and optical sideband filtering," *IEEE Photon. Technol. Lett.*, vol. 29, no. 11, pp. 917–920, Jun. 2017.

[28] A. M. Weiner, "Ultrafast optical pulse shaping: A tutorial review," *Opt. Commun.*, vol. 284, no. 15, pp. 3669–3692, Jul. 2011.

[29] X. Y. Han, E. M. Xu, W. L. Liu, and J. P. Yao. "Tunable dual-passband microwave photonic filter using orthogonal polarization modulation," *IEEE Photon. Technol. Lett.*, vol. 27, no. 20, pp. 2209–2212, Oct. 2017.

[30] S. S. Kelkar, L. L. Grigsby, and J. Langsner, "An extension of Parseval's theorem and its use in calculating transient energy in the frequency domain," *IEEE Trans. Ind. Electron.*, vol. IE-30, no. 1, pp. 42–45, Feb. 1983.

[31] X.H. Zou, P. X. Li, W. Pan, and L. S. Yan, "Photonic microwave filters with ultra-high noise rejection [Invited]," *Chinese Opt. Lett.*, vol. 17, no. 3, pp. 1–6, Mar. 2019.

[32] "3rd Generation partnership project; technical specification group radio access network; terminal conformance specification; radio transmission and reception (TDD)," 3GPP TS 34.122 V11.13.0, Oct. 2016. [Online]. Available: https://portal.3gpp.org/desktopmodules/Specifications/SpecificationDetails.aspx?specificationId=2365

[33] E. Ahmed and A. M. Eltawil, "All-digital self-interference cancellation technique for full-duplex systems," *IEEE Trans. Wireless Commun.*, vol. 14, no. 7, pp. 3519–3532, Jul. 2015.

[34] Y. H. Zhang, L. S. Li, M. H. Bi, and S. L. Xiao, "Over-the-air in-band full-duplex system with hybrid RF optical and baseband digital self-interference cancellation," *Opt. Commun.*, vol. 405, pp. 152–156, Jul. 2017.